Analysis of Zero-Reference-Pressure EoS/G^E Models

Nikolaos S. Kalospiros, Nikolaos Tzouvaras, Philippos Coutsikos, and Dimitrios P. Tassios
Lab. Thermodynamics and Transport Phenomena, Dept. of Chemical Engineering,
National Technical University of Athens, 15780 Athens, Greece

An analysis of EoS/G^E models, which are based on matching the EoS-derived expression for the excess Gibbs free energy G^E with that from a G^E model at zero pressure, is presented, with the focus on the most successful and widely used of these models, MHV2 and PSRK. It shows why zero-reference-pressure models do not reproduce exactly the G^E models at zero pressure and the ensuing implications on the prediction of asymmetric systems. The development of EoS/G^E models that reproduce exactly the G^E model is discussed. However, such reproducibility at zero pressure is impossible for systems containing components with reduced temperatures higher than about 0.9. Therefore, extrapolation schemes that allow treatment of such systems are examined.

Introduction

In an effort to extend the applicability of simple equations of state (EoS) to complex systems, several EoS/G^E models (G^E: excess Gibbs free energy) have been developed recently [Vidal, 1978; MHV1 and MHV2 (Michelsen, 1990b; Dahl and Michelsen, 1990); PSRK (Holderbaum and Gmehling, 1991); and LCVM (Boukouvalas et al., 1994)]. The main feature in the development of these models is to obtain the mixing rule for the mixture attractive-term parameter, a, of the EoS by setting the expression for G^E obtained from the EoS equal to that of an existing G^E-model; for example, UNIFAC, ASOG, NRTL. In the case of the Vidal model, this matching was postulated at infinite pressure. On the other hand, Michelsen (1990a) developed an EoS/G^E model by matching exactly the excess Gibbs free energy from the EoS to that of an existing G^E model at zero pressure, and is hereafter referred to as the "exact" model. The resulting mixing rule can be solved implicitly for the reduced attractive-term parameter, $\alpha = a/(bRT)$, of the mixture and has the following form:

$$\left(\frac{G^E}{RT}\right)^* + \sum x_i \ln\left(\frac{b}{b_i}\right) = q^e(\alpha) - \sum x_i q_i^e(\alpha_i); \quad (1)$$

$$q^e(\alpha) = -1 - \ln(u_0 - 1) - \frac{\alpha}{c_2 - c_1} \ln\left(\frac{u_0 + c_2}{u_0 + c_1}\right), \quad (2)$$

where $(G^E/RT)^*$ is obtained from a G^E model, x_i is the mixture composition, and $u = V/b$ a reduced volume. The mixture covolume parameter b is assumed to be equal to $b = \Sigma x_i b_i$. The subscript 0 denotes that u_0 refers to zero pressure; c_1 and c_2 are EoS-dependent parameters (for SRK, $c_1 = 0$, $c_2 = 1$; for PR, $c_1 = 1 - 2^{0.5}$, $c_2 = 1 + 2^{0.5}$; and for vdW, $c_1 = c_2 = 0$).

An important point is that the "exact" model cannot be applied to systems where one of the pure-component (and/or mixture) α-values is lower than a limiting α-value, α_{lim} (equal to $3 + 2^{0.5}$ for the SRK EoS; $4 + 2^{0.5}$ for PR; and 4 for vdW), since cubic EoS yield no real roots for the reduced volume u_0 for such α-values. In order to extend the applicability of this model to $\alpha < \alpha_{\text{lim}}$, several modifications of the exact model have been proposed, the main feature of which is the replacement of $q^e(\alpha)$ with an approximating function $q(\alpha)$, which in addition leads to an explicit mixing rule for α. PSRK and MHV1 assume a linear $q(\alpha)$ function, whereas MHV2 uses a quadratic form. Soave (1992) assumed a more complicated $q(\alpha)$ form. All these modifications are used in this article in the same fashion as proposed in their original development; that is, the same G^E model, EoS, and pure-component parameters are utilized. Finally, LCVM is a linear

Correspondence concerning this article should be addressed to D. P. Tassios.

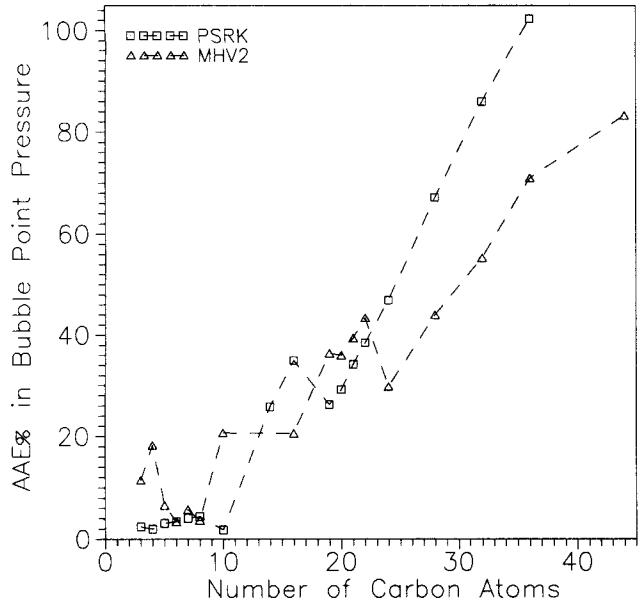

Figure 1. Average abs. % error in BUBL P vs. number of carbon atoms in the *n*-alkane obtained by various EoS/G^E models for carbon dioxide/*n*-alkane systems.

From Boukouvalas et al. (1994).

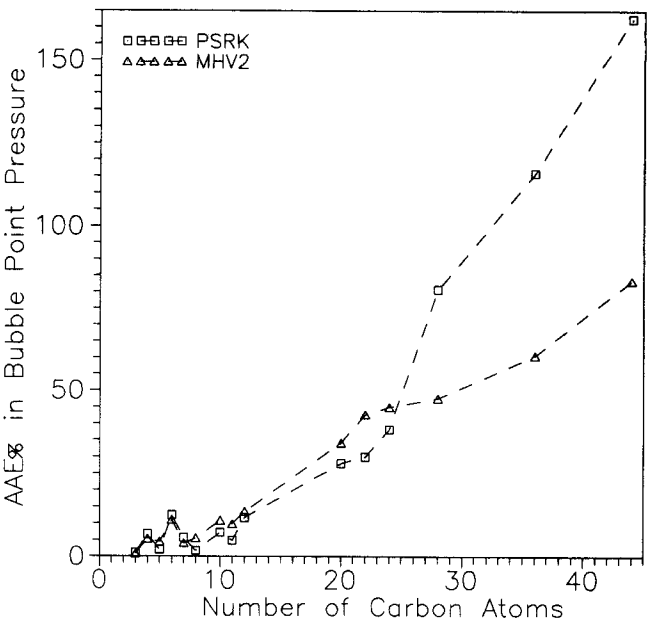

Figure 2. Average abs. % error in BUBL P vs. number of carbon atoms in the *n*-alkane obtained by various EoS/G^E models for ethane/*n*-alkane systems.

From Boukouvalas et al. (1994).

combination of the mixing rules of the Vidal and MHV1 models developed so as to give satisfactory bubble point pressure predictions for a variety of systems and has no specified reference pressure. In this article, we concentrate on the zero-reference-pressure EoS/G^E models, and especially the most successful and extensively used ones: MHV2 and PSRK.

Although MHV2 and PSRK have been quite successful in the prediction of vapor-liquid equilibrium (VLE) in systems with components of similar size (see, for example, Table 1), both models perform poorly when applied to systems with components that differ appreciably in size, such as those containing gases (ethane, carbon dioxide, or methane) with large *n*-alkanes. Some typical examples that demonstrate this type of behavior are shown in Figures 1 and 2, where plots of the average absolute % error in the predicted bubble point pressure (BUBL P) as a function of the carbon number of the alkane, N_C, for carbon dioxide/*n*-alkane and ethane/*n*-alkane systems, respectively, are shown. Note that in order to avoid the effect of erroneous *n*-alkane critical-property data, the critical temperature and pressure values as well as acentric factors critically evaluated and proposed by Magoulas and Tassios (1990) are used. It is evident that as the size difference increases, the results for PSRK and MHV2 become progressively poorer, and for N_C larger than 15–20, these models yield unacceptable predictions. Moreover, the failure of PSRK and MHV2 with increasing size difference is also demonstrated by their inability to arrive at a pair of interaction parameters of the G^E model that provide satisfactory results for the ethane/, and carbon dioxide/*n*-alkane binary mixtures (Spiliotis and Boukouvalas, 1993).

The objective of this study is to identify the capabilities and limitations of the zero-reference-pressure EoS/G^E models and explore ways of improving their performance. The remainder of the article is organized as follows: in the first part, we compare the G^E predictions obtained from the

Table 1. Symmetric and Weakly Asymmetric Systems Using MHV2 and PSRK EoS/G^E Models*

System	T, K	P, bar	V_{c1}/V_{c2}	MHV2		PSRK	
				ΔP**	Δy_1†	ΔP	Δy_1
Acetone/Chloroform‡	333–336	1.0	0.9	6.0	9.0	1.8	7.0
Benzene/Methyl Acetate§	330–350	1.0	1.1	4.1	9.0	1.1	6.0
Ethane/*n*-Propane‖	255	3.0–14	0.7	2.4	—	1.6	—
Ethane/*n*-Butane#	270	2.0–20	0.6	7.4	—	10	—

*The ratio of critical volumes, V_{c1}/V_{c2}, represents a measure of the asymmetry of the system.
**% abs. avg. dev. in BUBL P.
†Avg. dev. (×1,000) in mole fraction of component 1.
‡Hala et al. (1968).
§Nagata (1962).
‖Matschke and Thodos (1962).
#Clark and Stead (1988).

MHV2 and PSRK models with those from the G^E models used in their development, provide a theoretical analysis for the observed disagreement and illustrate the implications of increased asymmetry in the system components. In the second part, we examine the behavior of an EoS/G^E model, which at zero pressure exactly reproduces the G^E model it is combined with. Since such a model is not defined for systems containing a light component with reduced temperature higher than 0.9, we examine, in the third part, ways of extrapolating this model to VLE prediction of such systems and test their performance in BUBL P predictions of asymmetric mixtures. No extrapolation scheme seems to work successfully if the G^E model is to be reproduced exactly for $\alpha > \alpha_{lim}$, suggesting that a model that can yield successful VLE predictions may have to sacrifice the reproducibility of the G^E model. We close with our conclusions.

The G^E Expression from EoS/G^E Models

Comparison of excess Gibbs-free-energy predictions by EoS/G^E and G^E models

In the present section, we compare the excess Gibbs free energy obtained by PSRK and MHV2 models with the values predicted by the G^E models used in their development. The activity coefficient of component i in a mixture, as predicted by any one of the aforementioned models, is simply calculated as

$$\gamma_i = \hat{\varphi}_i/\varphi_i$$

where $\hat{\varphi}_i$ is the fugacity coefficient of component i in the mixture, and φ_i is the fugacity coefficient of pure component i at the temperature and pressure of the mixture. Subsequently, G^E is calculated as the sum

$$\frac{G^E}{RT} = \sum x_i \ln \gamma_i$$

with x_i denoting the mixture composition.

In Figures 3 and 4, we present G^E predictions with zero-reference-pressure EoS/G^E models (PSRK and MHV2) for systems of varying degrees of asymmetry. (A measure of this degree is the ratio of the critical volumes of the pure components). Figure 3 contains the results for the system acetone (1)/benzene (2) at 318.15 K and 0.1 bar ($V_{C1}/V_{C2} = 0.8$). The zero-reference-pressure models reproduce *closely*, though *not exactly*, the G^E model they are combined with (original UNIFAC for PSRK; modified UNIFAC for MHV2), in agreement with Michelsen's statement (Michelsen, 1990b) for the MHV2 model and for systems where the α values of the components are in the range used to obtain the parameters of the quadratic $q(\alpha)$ form ($\alpha = 10$–13). However, as the system asymmetry increases, the G^E models are not reproduced by the EoS/G^E models considered here. This is shown in Figure 4 for n-hexane (1)/n-hexadecane (2) at 293.15 K and 0.1 bar ($V_{C1}/V_{C2} = 2.5$). Note that the differences in G^E cannot be attributed to the difference between the pressure value (0.1 bar) used to generate the results in Figures 3 and 4 and the zero reference pressure of the models. For such low pressure difference, negligible differences between the activity coefficients of the EoS/G^E models at zero pressure and pressure equal to 0.1 are expected.

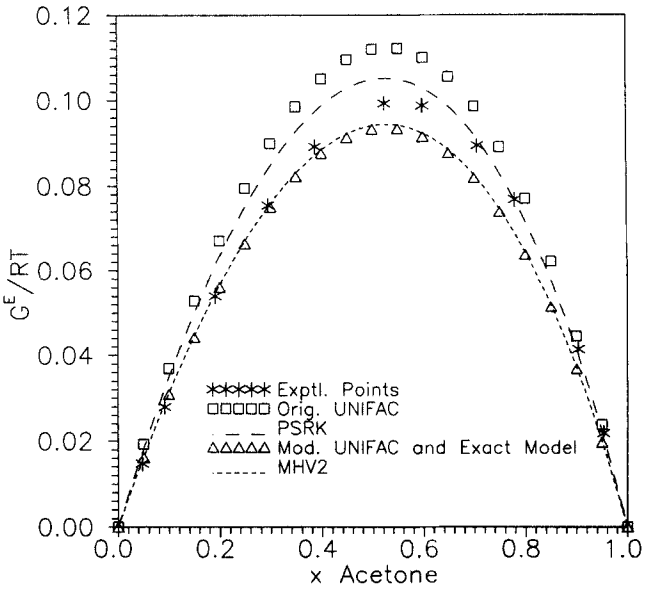

Figure 3. G^E/RT as a function of composition for the system acetone/benzene ($V_{c1}/V_{c2} = 0.8$) at 318.15 K and 0.1 bar.

The "exact" model is combined with the modified UNIFAC. Experimental data obtained from van Laar equation using the parameters of Hala et al. (1968).

The fact that the zero-reference-pressure models do not in general reproduce the G^E models they utilize suggests that the activity coefficients predicted by PSRK and MHV2 also do not reproduce the activity coefficients of the G^E models.

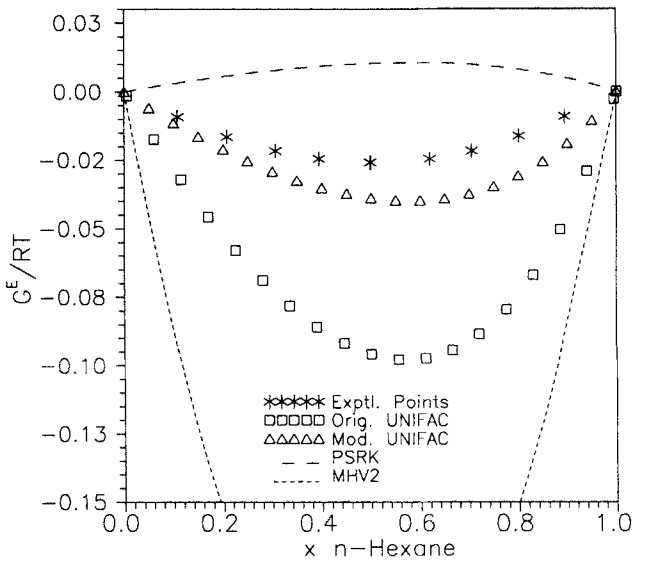

Figure 4. G^E/RT as a function of composition for the system n-hexane/n-hexadecane ($V_{c1}/V_{c2} = 2.5$) at 293.15 K and 1 bar.

Experimental data from Shen Weiguo et al. (1990).

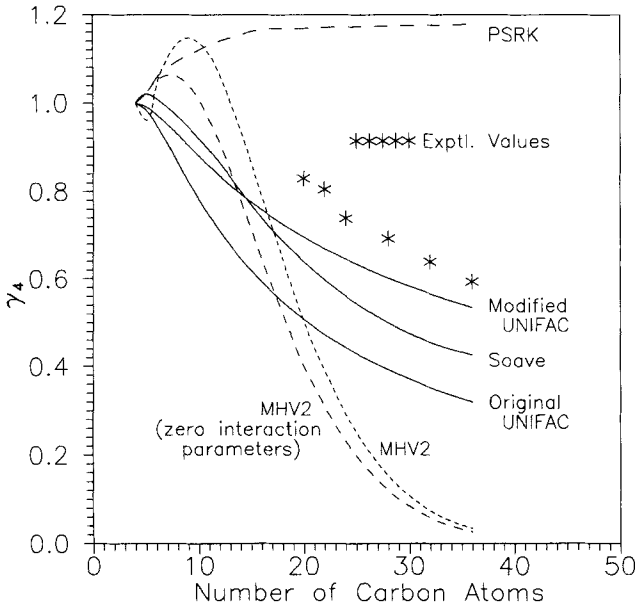

Figure 5. Infinite dilution activity coefficient of *n*-butane in *n*-alkanes at 373.15 K and 1 bar as a function of the number of carbon atoms in the *n*-alkane.

Experimental data from Parcher et al. (1975).

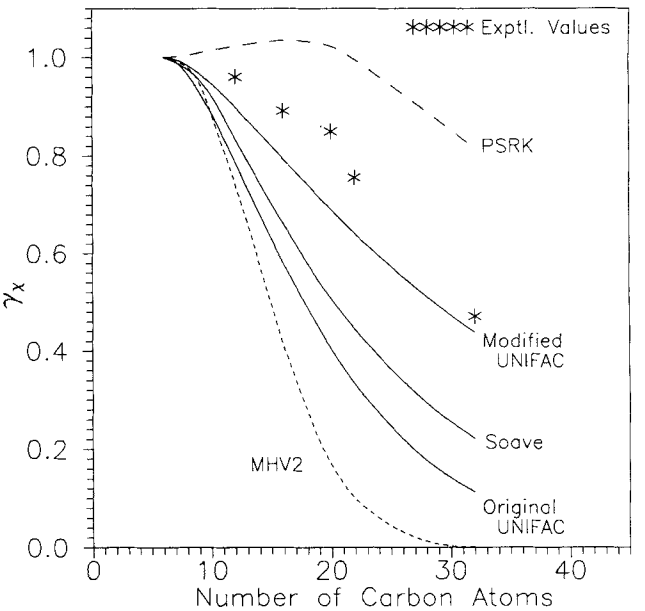

Figure 6. Infinite dilution activity coefficient of *n*-alkanes in *n*-hexane at 273.15 K and 1 bar as a function of the number of carbon atoms in the *n*-alkane.

Experimental data from Kniaz (1991) at temperatures approximately equal to 273.15 K.

This is demonstrated in Figures 5 and 6, where infinite dilution activity coefficients of *n*-butane in *n*-alkanes and *n*-alkanes in *n*-hexane, respectively, as a function of the carbon number, N_C, are plotted. Notice that both PSRK and MHV2 fail to reproduce the activity coefficient behavior predicted by the G^E model used—original UNIFAC (Hansen et al., 1991) for PSRK and modified UNIFAC (Larsen et al., 1987) for MHV2—with the relative difference between γ_i predicted by the EoS and the G^E model increasing with N_C. A predicament of both PSRK and MHV2 is that they may yield activity coefficients slightly larger than unity at small N_C, in disagreement with the G^E models they are combined with.

Theoretical explanation

It can be shown (see Appendix) that the difference $\Delta \ln \gamma_i$, between the logarithm of the activity coefficient predicted by an EoS/G^E model and the corresponding quantity $\ln \gamma_i^*$ of the G^E model used, is at zero pressure

$$\Delta \ln \gamma_i = -(\alpha - \bar{\alpha}_i)\left[\frac{dq^e(\alpha)}{d\alpha} - \frac{dq(\alpha)}{d\alpha}\right] + [q^e(\alpha) - q(\alpha)] - [q^e(\alpha_i) - q(\alpha_i)]. \quad (3)$$

The corresponding excess Gibbs-free-energy difference is given by

$$\Delta\left(\frac{G^E}{RT}\right) = \left(\frac{G^E}{RT}\right) - \left(\frac{G^E}{RT}\right)^* = [q^e(\alpha) - q(\alpha)] - \sum x_i[q^e(\alpha_i) - q(\alpha_i)], \quad (4)$$

where $q(\alpha)$ is the approximating function used by any EoS/G^E model of the exact form $q^e(\alpha)$ (Eq. 2), and $dq(\alpha)/d\alpha$, $dq^e(\alpha)/d\alpha$ are the respective slopes. Note that Eqs. 1 and 2 hold for all EoS/G^E models with zero reference pressure.

The preceding equations lead to the following comments regarding the performance of zero-reference-pressure EoS/G^E models.

(1) Equation 4 demonstrates that these models, by assuming an approximate form $q(\alpha)$ for $q^e(\alpha)$, do not, in general, reproduce the G^E model; that is, these models do not actually have a true zero reference pressure. They can only approximately reproduce the G^E models, and how good this approximation is depends on the difference between $q^e(\alpha)$ and $q(\alpha)$, and $q^e(\alpha_i)$ and $q(\alpha_i)$. More specifically, the form of Eq. (4) suggests that $q(\alpha)$ and $q^e(\alpha)$ need only be equal to within an additive constant. In Figure 7, the approximate forms $q(\alpha)$, assumed in the development of the PSRK, MHV1, and MHV2 models, along with the exact form $q^e(\alpha)$ are plotted as functions of α using the SRK EoS. For MHV1 and MHV2, $q^e(\alpha)$ was fitted in the α-range between 10 and 13 to a linear and quadratic function, respectively (Michelsen, 1990b). Soave (1992), however, observed that the quadratic approximation of MHV2 describes the $q^e(\alpha)$ curve accurately within ± 0.01 in the range $\alpha = 8$–18. For PSRK, the chosen value of the slope of the linear approximate form $q(\alpha)$ corresponds to the slope of $q^e(\alpha)$ at an α-value approximately equal to 23 (Holderbaum and Gmehling, 1991).

(2) From the preceding comment it is obvious that a better description of $q^e(\alpha)$ with an approximate form $q(\alpha)$ in a wide range of α values would suffice to reproduce closely

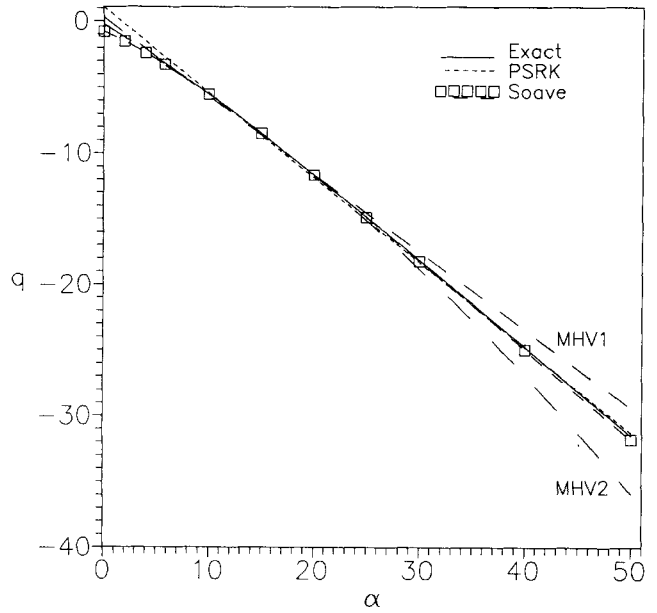

Figure 7. $q^e(\alpha)$ and approximating functions $q(\alpha)$ vs. α with the SRK EoS.

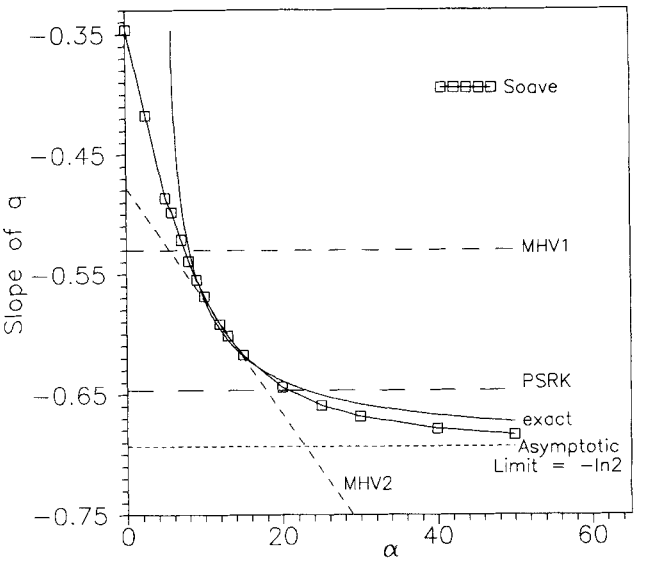

Figure 8. $dq^e(\alpha)/d\alpha$ and $dq(\alpha)/d\alpha$ of various models vs. α with the SRK EoS.

the G^E model. For example, a quadratic fit of $q^e(\alpha)$ in a wider range of α's could improve the agreement between the G^E/RT obtained from MHV2 and the modified UNIFAC. However, even exact reproduction of the G^E/RT of the G^E model does not necessarily imply the same for the activity coefficients. The theoretical explanation of this effect is provided by Eq. 3, where it is shown that $\Delta \ln \gamma_i$ does not only depend on the goodness of the fit of $q^e(\alpha)$ with an appropriate $q(\alpha)$ but also on the difference between the corresponding derivatives $dq^e(\alpha)/d\alpha$ and $dq(\alpha)/d\alpha$. Examples of this behavior are given in Figures 5 and 6 for the infinite dilution activity coefficient of *n*-butane in *n*-alkanes and *n*-alkanes in *n*-hexane, respectively. Specifically, although all models reproduce the G^E model exactly at the infinite dilution limit [since $G^E/RT = (G^E/RT)^* = 0$], this is not the case with γ_i^∞.

(3) A plot of the derivatives $dq(\alpha)/d\alpha$ for PSRK, MHV1, and MHV2 models along with $dq^e(\alpha)/d\alpha$ as functions of α is presented in Figure 8 for the SRK EoS. Notice that all three models provide a very poor approximation of the derivative $dq^e(\alpha)/d\alpha$; that is, the small differences observed in Figure 7 now become very large. Note also that the approximation will remain poor regardless of the goodness of the fit for $q^e(\alpha)$, as long as a quadratic or linear form for $q(\alpha)$ is used. As a result, for wide ranges of the mixture parameter α, a large difference $[dq^e(\alpha)/d\alpha - dq(\alpha)/d\alpha]$ appears that can have a significant effect on $\Delta \ln \gamma_i$. On the other hand, there are ranges of α where the difference $[dq^e(\alpha)/d\alpha - dq(\alpha)/d\alpha]$ is quite small (Figure 8). For MHV1, this range is approximately the one where the fit of $q^e(\alpha)$ took place ($\alpha = 10$–13), while for MHV2, the range of good representation of $dq^e(\alpha)/d\alpha$ is in the α-range between 8 and 18. For PSRK, the range of good agreement between $dq^e(\alpha)/d\alpha$ and $dq(\alpha)/d\alpha$ is in the region of α equal to approximately 23, since the slope in the linear $q(\alpha)$-form of PSRK corresponds to this value.

(4) The preceding discussion leads to the conclusion that the zero-reference-pressure models may approximately reproduce the G^E model they are combined with only for systems that fulfill the following requirement:

The components of these binaries are characterized by α_i values, which are in the α-range, where $q^e(\alpha)$ and $dq^e(\alpha)/d\alpha$ are described satisfactorily by the approximate $q(\alpha)$ and $dq(\alpha)/d\alpha$ forms (10–13 for MHV1; 8–18 for MHV2; 20–25 for PSRK). Consequently, the mixture α is also in the same range.

This requirement ensures close reproduction of the excess Gibbs free energy of the G^E model (small $[q^e(\alpha) - q(\alpha)]$ differences) and also low $[dq^e(\alpha)/d\alpha - dq(\alpha)/d\alpha]$ values. Reproduction of the activity coefficients follows from the small $[dq^e(\alpha)/d\alpha - dq(\alpha)/d\alpha]$ values, provided that the coefficient $\alpha - \bar{\alpha}_i$ is not excessively large (see item 6 below). When the previous requirement is largely violated, the degree to which the G^E from the EoS/G^E model differs from that of a G^E model is rather a matter of cancellation between the differences in the righthand sides of Eqs. 3 and 4. Finally, note that for an ideal system with $\alpha_i = \alpha_j$ (for which the mixture α is equal to the pure component α_i's), both $\Delta \ln \gamma_i$ and $\Delta(G^E/RT)$ of Eqs. 3 and 4 are identically zero, regardless of the α-range used to fit $q^e(\alpha)$. In this special case, the slope difference is unimportant, since the coefficient $\alpha - \bar{\alpha}_i$ will be identically zero.

(5) The discussion under item 4 suggests that in the context of zero-reference-pressure EoS/G^E models, *a symmetric system is a mixture containing components characterized by similar α_i values, rather than molecular sizes or critical volumes* (the definition used in Table 1). However, even for such systems, approximate reproduction of the G^E model is guaranteed when the pure component and mixture α-values are in a specific range. Under the same prism, an ideal mixture with α_i's equal to each other can be then considered as a "completely symmetric" system. It is only in this case that the G^E model is exactly reproduced.

(6) A comment regarding the fashion in which the asymmetry of the system is taken into account in Eq. 3 is now in order. The coefficient of the $[dq^e(\alpha)/d\alpha - dq(\alpha)/d\alpha]$ term in Eq. 3, $\alpha - \bar{\alpha}_i$, is a measure of the asymmetry of the system. The larger the difference in the size of the components of the mixture, the larger the value of $\alpha - \bar{\alpha}_i$. Consequently, in this case even a small difference between $dq^e(\alpha)/d\alpha$ and $dq(\alpha)/d\alpha$ can result in a significantly large effect on $\Delta \ln \gamma_i$. This is the main reason why the difference $\Delta \ln \gamma_i$ increases with the carbon number of *n*-alkanes in Figures 5 and 6.

(7) Consideration of Soave's model provides a justification of the discussion in the preceding entries. Specifically, Figures 7 and 8 show that Soave's approximation for $q^e(\alpha)$ provides not only a good fit of $q^e(\alpha)$ but also a reasonably good representation of $dq^e(\alpha)/d\alpha$ over the entire α-range. Consequently, this model is expected to yield activity coefficients closer to the ones of the G^E model it is combined with (modified UNIFAC), even for highly asymmetric systems. Indeed, this is shown to be the case with the results of infinite dilution activity coefficients of *n*-butane in *n*-alkanes (Figure 5) and *n*-alkanes in *n*-hexane (Figure 6). Notice that the Soave model's results are in much better agreement with the modified UNIFAC G^E model than MHV2.

Exact Model

In the last section, we demonstrated theoretically that EoS/G^E models such as PSRK, MHV1, and MHV2 do not reproduce the G^E model (original or modified UNIFAC) they are associated with at zero pressure due to the differences in the values and the corresponding derivatives of the exact form $q^e(\alpha)$ and the approximating function $q(\alpha)$ assumed in the development of these models. On the other hand, the exact model, briefly described in the Introduction, reproduces *exactly* both the excess Gibbs free energy and the activity coefficients of the G^E model at zero pressure; that is, $\Delta \ln \gamma_i$ and $\Delta(G^E/RT)$ in Eqs. 3 and 4 are identically zero (see Figure 3), but cannot be applied to systems with α's of the components (and/or the mixture) lower than a limiting value α_{lim}. Next we examine the results obtained with the $\gamma - \hat{\varphi}$ approach, using the same G^E model for the activity coefficients. Extrapolation procedures to α's smaller than α_{lim} are discussed in the next section.

In Table 2, we present BUBL P results using these two approaches for several polar and nonpolar *n*-alkane/*n*-alkane systems at low pressures (up to 20 atm). The exact model is used in combination with the *t*-*m*PR equation of state (Magoulas and Tassios, 1990) and the original UNIFAC G^E model (Fredenslund et al., 1975; Hansen et al., 1991) for the polar systems, or the modified UNIFAC (Larsen et al., 1987) for the *n*-alkane/*n*-alkane ones, while the $\gamma - \hat{\varphi}$ approach uses the G^E model that the exact one is combined with, to describe the liquid phase, and the virial EoS truncated to the second term with second virial coefficients from Tsonopoulos' correlation (Tsonopoulos, 1974, 1975) to describe the vapor phase.

Note that the EoS/G^E-model approach gives practically the same results as the $\gamma - \hat{\varphi}$ one, even for the very asymmetric systems. This also suggests that, since the liquid-phase fugacity (and activity) coefficient values for the two approaches are similar, the same is the case for the vapor-phase ones, at least at low pressures. For example, the infinite dilution fugacity coefficient of *n*-dodecane in propane at 2.7 bar and 273 K is 0.71 and 0.75 as obtained by the exact model and the $\gamma - \hat{\varphi}$ approach, respectively. The respective values for *n*-eicosane in propane at 6.3 bar and 310 K are equal to 0.23 and 0.21.

Table 2. Polar and Nonpolar (*n*-Alkane/*n*-Alkane) Systems*

System	T, K	P, bar	"Exact"		$\gamma - \hat{\varphi}$	
			ΔP**	$\Delta y_1^\dagger$	ΔP	Δy_1
Acetone/Chloroform‡	333–336	1.0	3.3	8.8	2.7	8.5
Benzene/Methyl Acetate§	330–350	1.0	0.9	6.8	1.1	6.6
Methanol/Benzene‖	373	3.1–4.2	5.8	24	4.8	22
Ethanol/Water#	473	5.0–10	5.2	1.3	4.0	2.7
Methanol/Water††	373	1.0–3.4	2.3	12	2.1	10
Ethane/*n*-Propane‡‡	255	3.0–14	2.5	—	1.4	—
Ethane/*n*-Butane§§	270	2.0–20	2.3	—	4.0	—
Ethane/*n*-Octane‖‖	273	4.0–22	20	—	17	—
Ethane/*n*-Dodecane##	273	4.0–22	25	—	23	—
n-Propane/*n*-Eicosane***	310	4.0–22	17	—	16	—
n-Hexane/*n*-Hexadecane†††	298	0.0–0.2	3.5	—	1.5	—

*The "exact" model is used in combination with *t*-*m*PR EoS and original (Hansen et al., 1991) or modified UNIFAC (Larsen et al., 1987). The $\gamma - \hat{\varphi}$ approach utilizes the same version of UNIFAC as the "exact" model.
**ΔP: Percent absolute average deviation in BUBL P.
†Δy_1: Average deviation ($\times 1000$) in mole fraction of component 1.
‡Hala et al. (1968).
§Nagata (1962).
‖Butcher and Medani (1968).
#Barr-David and Dodge (1959).
††Griswold and Wong (1952).
‡‡Matschke and Thodos (1962).
§§Clark and Stead (1988).
‖‖Rodrigues et al. (1968).
##Legret et al. (1980).
***Gregorowicz et al. (1992).
†††Shen Weiguo et al. (1990).

Extrapolation Schemes of Exact Model

Exact-1 model

The next step is the development of EoS/G^E models that reproduce very closely the G^E model used for all types of systems and, additionally, provide with natural extrapolation to α values lower than α_{lim}, a range along which the exact model cannot be applied. From our previous discussion it is obvious that such models should describe $q^e(\alpha)$ and $dq^e(\alpha)/d\alpha$ equally well for $\alpha > \alpha_{lim}$, so that both $(G^E/RT)^*$ and $\ln \gamma_i^*$ can be closely reproduced.

In order to develop such a model, the derivative $dq^e(\alpha)/d\alpha$ is fitted to a function of the form

$$\frac{dq(\alpha)}{d\alpha} = -\frac{k_1}{\alpha^n} + k_0 e^{-\alpha} + s_\infty, \qquad (5)$$

where k_0, k_1, n are positive numbers and s_∞ is the infinite slope ($\alpha \to \infty$) for the derivative $dq^e(\alpha)/d\alpha$ (approximately equal to -0.623 for the *t-m*PR EoS). The resulting parameters are $k_0 = 71$, $k_1 = 1.847$, and $n = 1.161$ and provide excellent fit for $dq^e(\alpha)/d\alpha$ of the *t-m*PR EoS. The quality of the fit is slightly poorer in the region of α_{lim}, so as to allow extrapolation of $dq(\alpha)/d\alpha$ to α-values lower than α_{lim}.

Integration of Eq. (5) yields

$$q(\alpha) = -\frac{k_1}{n-1} \cdot \frac{1}{\alpha^{n-1}} - k_0 \cdot e^{-\alpha} + s_\infty \cdot \alpha + q_0. \qquad (6)$$

Note that the value of q_0 plays no role in BUBL P and γ (or G^E) calculations. Nonetheless, we have fitted q_0 to obtain the best agreement between $q^e(\alpha)$ and $q(\alpha)$ ($q_0 = 9.271$). Note that $q(\alpha)$ presents a maximum for an α-value approximately equal to 5 (with $\alpha_{lim} = 6.84$ for *t-m*PR EoS). The function $q(\alpha)$ defined by Eq. (6) can be used in cases where the exact model is not applied. The resulting mixing rule is implicit with respect to α of the mixture and has the same form as Eq. 1 with $q(\alpha)$ from Eq. 6 in place of $q^e(\alpha)$. The mixture b-parameter is given as a linear combination of b_i's. This mixing rule is used in combination with the *t-m*PR EoS and original or modified UNIFAC, and is referred to as the exact-1 model.

At first, this model is applied to the systems examined in the last section, for which the exact model is applicable. Nearly identical results are obtained with the exact model, since $q(\alpha)$ and $q^e(\alpha)$, along with the corresponding derivatives, are in close agreement with each other, and the detailed results are thus not shown in Table 2. The predicted activity coefficients using the exact-1 model are also expected to be nearly identical with the exact model (and the G^E model at low to moderate pressures) results, since the present model was designed taking this agreement into account.

The behavior of the exact-1 model at ethane/*n*-alkane systems, where the α-parameter of the ethane and/or the mixture is smaller than α_{lim}, is shown in Figure 9. The model was combined with modified UNIFAC using zero interaction parameters. The results demonstrate that the extrapolation to low α-values provided by Eq. 6 collapses ($\Delta P \geq 30\%$) even for the system ethane/*n*-pentane and in general deteriorate as the system asymmetry increases. A very similar behavior is shown in Table 2 with the BUBL P results of the exact model for ethane/*n*-alkane systems. In both cases, the poor results as the system asymmetry increases are attributed to the inability of the G^E model to describe satisfactorily the liquid phase of these mixtures.

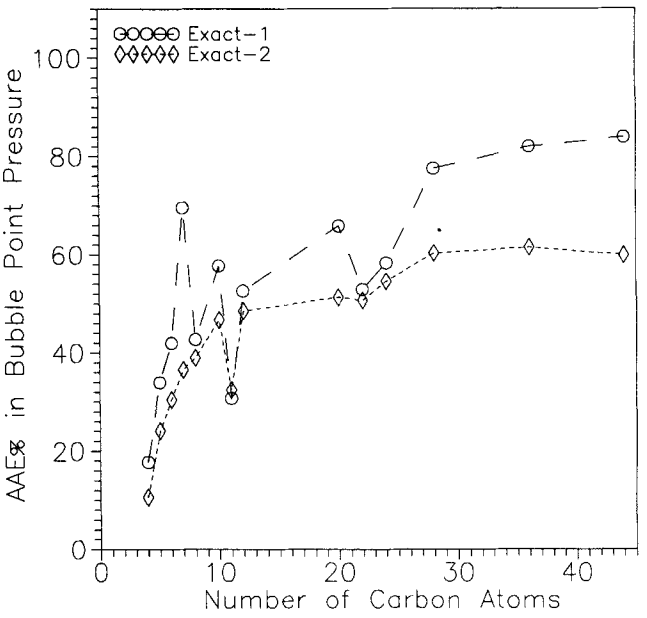

Figure 9. Average abs. % error in BUBL P vs. number of carbon atoms in the *n*-alkane obtained by the exact-1 and exact-2 models for ethane/*n*-alkane systems.

Zero interaction parameters are used in the modified UNIFAC. $\alpha_{cut} = 6.88$ for the exact-2 model.

Exact-2 model

A different extrapolation scheme to $\alpha < \alpha_{lim}$ is in order now, which is also examined with respect to BUBL P predictions for highly asymmetric systems. Specifically, the mixing rule of the exact model is used down to an α-value equal to $\alpha_{cut} > \alpha_{lim}$. For α's lower than α_{cut}, a quadratic extrapolation of the form (Michelsen, 1990a)

$$\alpha = \alpha_{cut} + k_1(q - q_{cut}) + k_2(q - q_{cut})^2 \qquad (7)$$

is used to evaluate q. At $\alpha = \alpha_{cut}$, $q^e(\alpha_{cut}) = q(\alpha_{cut}) = q_{cut}$. Also, k_1 and k_2 are calculated so that $\alpha = \alpha_{cut}$.

$$\left[\frac{dq}{d\alpha}\right] = \left[\frac{dq^e}{d\alpha}\right] \quad \text{and} \quad \left[\frac{dq^2}{d\alpha^2}\right] = \left[\frac{d^2q^e}{d\alpha^2}\right]. \qquad (8)$$

This model is referred to as exact 2.

At first, α_{cut} is chosen to be close to α_{lim} ($\alpha_{cut} = 6.88$; $\alpha_{lim} = 6.85$), so that this model coincides with exact 1 for essentially all α's above α_{lim}. For *t-m*PR EoS with $\alpha_{cut} = 6.88$, we obtain $q_{cut} = -3.491$, $k_1 = -2.9458$, and $k_2 = -3.4235$. Using the preceding mixing rule when extrapolation to small α-values is required, the results shown in Figure 9 are ob-

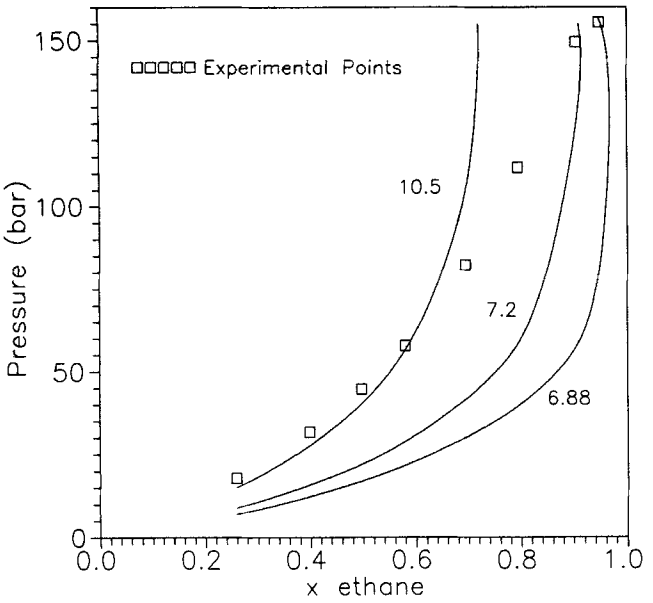

Figure 10. Effect of α_{cut} on BUBL P predictions obtained with the exact-2 model for the system ethane/*n*-eicosane at 380 K.

tained for the ethane/*n*-alkane database. The predictions are in general better than the exact-1 model's predictions, but still unacceptable.

In Figure 10, the effect of α_{cut} in the BUBL P predictions for the system ethane/*n*-eicosane at 380 K is demonstrated. Notice that the experimental behavior cannot be approached, regardless of the α_{cut} value. These results along with the discussion on the exact-1 model suggest that no extrapolation scheme performs successfully if the G^E model is to be reproduced exactly, even at a small range of α-values.

Conclusions

The analysis presented in this paper shows that the zero-reference-pressure EoS/G^E models PSRK, MHV1, and MHV2 do not in general reproduce the G^E model used in their development for the whole range of α values. Approximate reproduction is guaranteed only for systems with pure components characterized by similar α_i's, which are in the model-dependent α-range. Such systems can be considered as *symmetric systems* in the context of these EoS/G^E models. As the degree of asymmetry increases (large difference between α_i's of the pure components), the reproducibility of the G^E model and the corresponding activity coefficients become poorer, depending on the difference of the exact and approximating $q(\alpha)$ functions and the respective derivatives.

Exact description of the $q(\alpha)$ curve leads to the exact model and results in exact reproducibility of the excess Gibbs free energy and the activity coefficients of the G^E model, but cannot be extrapolated to α's lower than a limiting value, α_{lim}. Attempts to provide extrapolation schemes of the exact model did not give good results, suggesting that a model is necessary that upon sacrificing the exact G^E model reproducibility, will provide good BUBL P prediction and possibly yield an EoS/G^E-derived G^E expression close to the experimental one at low pressures. The LCVM model of Boukouvalas et al. (1993), an EoS/G^E model that is a linear combination of the mixing rules of the Vidal and MHV1 models and has no specified reference pressure, represents a first approximation to such an approach.

Notation

a = attractive-term parameter in EoS (bar·cm^6/mol^2)
b = covolume parameter in EoS (cm^3/mol)
c_1, c_2 = EoS parameters in Eq. 2
f = fugacity (bar)
k_0, k_1, k_2 = parameters of exact-1 and exact-2 EoS/G^E model
n = parameter of exact-1 EoS/G^E model and number of moles (mol)
N_C = carbon number of a *n*-alkane
P = pressure (bar)
$q(\alpha)$ = approximating function of $q^e(\alpha)$
$q^e(\alpha)$ = exact function, defined by Eq. 2
R = ideal gas constant (= 8.314 J/(mol K))
s_∞ = infinite-α slope of $q^e(\alpha)$ ($-\ln 2$ for SRK and -0.623 for *t*-*m*PR EoS)
T = temperature (K)
$u = V/b$
V = molar volume (cm^3/mol)
x = mixture composition

Greek letters

$\alpha = a/(bRT)$
α_{lim} = limiting value for which $q^e(\alpha)$ is defined
$\bar{\alpha}_i$ = partial molar α
γ = activity coefficient
Δ = difference between EoS/G^E model and G^E model values
ΔP = % absolute average deviation in BUBL P prediction
Δy_1 = average deviation ($\times$1,000) in mole fraction of component 1
φ = fugacity coefficient

Subscripts and superscripts

0 = at zero pressure
c = critical property
i, j = component in a mixture
$*$ = referring to a G^E model

Literature Cited

Barr-David, F., and B. F. Dodge, "Vapor-Liquid Equilibrium at High Pressures. The Systems Ethanol-Water and 2-Propanol-Water," *J. Chem. Eng. Data*, **4**, 107 (1959).

Boukouvalas, C., N. Spiliotis, Ph. Coutsikos, N. Tzouvaras, and D. Tassios, "Prediction of Vapor-Liquid Equilibrium with the LCVM Model: A Linear Combination of the Vidal and Michelsen Mixing Rules Coupled with the Original UNIFAC and the t-mPR Equation of State," *Fluid Phase Equil.*, **92**, 75 (1994).

Butcher, K. L., and M. S. Medani, "Thermodynamic Properties of Methanol-Benzene Mixtures at Elevated Temperatures," *J. Appl. Chem.*, **18**, 100 (1968).

Clark, A., and K. Stead, "(Vapour + Liquid) Phase Equilibria at Binary, Ternary and Quaternary Mixtures of CH_4, C_2H_6, C_3H_8, C_4H_{10}, and CO_2," *J. Chem. Thermody.*, **20**, 413 (1988).

Dahl, S., and M. L. Michelsen, "High-Pressure Vapor-Liquid Equilibrium with a UNIFAC-Based Equation of State," *AIChE J.*, **36**, 1829 (1990).

Fredenslund, Aa., R. L. Jones, and J. M. Prausnitz, "Group-Contribution Estimation of Activity Coefficients in Nonideal Liquid Mixtures," *AIChE J.*, **21**, 1086 (1975).

Gregorowicz, J., T. W. de Loos, and J. de Swaan Arons, "The System Propane + Eicosane: P, T, Mixture Component Measurements In the Temperature Range 288–358 K," *J. Chem. Eng. Data*, **37**, 356 (1992).

Griswold, J., and S. Y. Wong, "Phase Equilibria of the Acetone-Methanol-Water System from 100°C into the Critical Region," *AIChE Symp. Ser.*, **48**, 18 (1952).

Hansen, H. K., P. Rasmussen, Aa. Fredenslund, M. Schiller, and J. Gmehling, "Vapor-Liquid Equilibria by UNIFAC Group-Contribution. 5. Revision and Extension," *SEP 9101*, Institut for Kemiteknik, DTH, Lyngby, Denmark (1991).

Hala, E., I. Wichterle, J. Polak, and T. Boublik, *Vapour Liquid Equilibrium Data at Normal Pressures*, Pergamon, London (1968).

Holderbaum, T., and J. Gmehling, "A Group Contribution Equation of State Based on UNIFAC," *Fluid Phase Equil.*, **70**, 251 (1991).

Kniaz, K., "Influence of Size and Shape Effects on the Solubility of Hydrocarbons: The Role of the Combinatorial Entropy," *Fluid Phase Equil.*, **68**, 35 (1991).

Larsen, B. L., P. Rasmussen, and Aa. Fredenslund, "A Modified UNIFAC Group-Contribution Model for Prediction of Phase Equilibria and Heats of Mixing," *Ind. Eng. Chem. Res.*, **26**, 2274 (1987).

Legret, D., D. Richon, and H. Renon, "Static Still for Measuring Vapor-Liquid Equilibria Up to 50 bar," *Ind. Eng. Chem. Fundam.*, **19**, 122 (1980).

Magoulas, K., and D. Tassios, "Thermophysical Properties of *n*-Alkanes from C1 to C20 and Their Prediction for Higher Ones," *Fluid Phase Equil.*, **56**, 119 (1990).

Matschke, D., and G. Thodos, "Vapor-Liquid Equilibria of the Ethane-Propane System," *J. Chem. Eng. Data*, **7**, 232 (1962).

Michelsen, M. L., "A Method for Incorporating Excess Gibbs Energy Models in Equations of State," *Fluid Phase Equil.*, **60**, 47 (1990a).

Michelsen, M. L., "A Modified Huron-Vidal Mixing Rule for Cubic Equations of State," *Fluid Phase Equil.*, **60**, 213 (1990b).

Nagata, I., "Vapor Liquid Equilibrium at Atmospheric Pressure for the Ternary System, Methyl Acetate-Chloroform-Benzene," *J. Chem. Eng. Data*, **7**, 360 (1962).

Parcher, J. F., P. H. Weiner, C. L. Hussey, and T. N. Westlake, "Specific Retention Volumes and Limiting Activity Coefficients of C_4–C_8 *n*-Alkane Solutes in C_{22}–C_{36} *n*-Alkane Solvents," *J. Chem. Eng. Data*, **20**, 145 (1975).

Rodriguez, A. B. J., D. S. McCaffrey, and J. P. Kohn, "Heterogeneous Phase and Volumetric Equilibrium in the Ethane-*n*-Octane System," *J. Chem. Eng. Data*, **13**, 164 (1968).

Shen Weiguo, An Xue Qin, P. J. McElroy, and A. G. Williamson, "(Vapour + Liquid) Equilibria of (*n*-Hexane + *n*-Hexadecane), (*n*-Hexane + *n*-Octane), and (*n*-Octane + *n*-Hexadecane)," *J. Chem. Thermody.*, **22**, 905 (1990).

Soave, G., "A New Expression of $q(\alpha)$ for the Modified Huron-Vidal Methods," *Fluid Phase Equil.*, **72**, 325 (1992).

Spiliotis, N., and C. Boukouvalas, "Solubilities of Liquids in Compressed Gases with Group-Contribution Methods," MS Thesis (in Greek), Nat. Technical Univ., Athens, Greece (1993).

Tsonopoulos, C., "An Empirical Correlation of Second Virial Coefficients," *AIChE J.*, **20**, 263 (1974).

Tsonopoulos, C., "Second Virial Coefficients of Polar Haloalkanes," *AIChE J.*, **21**, 827 (1975).

Vidal, J., "Mixing Rules and Excess Properties in Cubic Equations of State," *Chem. Eng. Sci.*, **33**, 787 (1978).

Appendix

Derivation of Eqs. 3 and 4

The activity coefficient, γ_i, of component i in the liquid phase of a mixture is defined as the ratio of the fugacity coefficient, $\hat{\varphi}_i$, of component i in the mixture and the fugacity coefficient, φ_i, of pure component i at the temperature, T, and pressure, P, of the mixture. Any one of the models (MHV1, MHV2, PSRK, or Soave's) can be used to obtain values of these fugacity coefficients, and consequently, calculate γ_i. The following relationship is obtained:

$$\ln \gamma_i = \ln \frac{\hat{\varphi}_i}{\varphi_i} = \frac{Pb_i}{RT}(u-u_i) - \left[\frac{b_i}{b} - 1 + \ln\left(\frac{b}{b_i}\right)\right] - \ln\left(\frac{u-1}{u_i-1}\right) - \frac{\overline{\alpha}_i}{c_2-c_1}\ln\left(\frac{u+c_2}{u+c_1}\right) + \frac{\alpha_i}{c_2-c_1}\ln\left(\frac{u_1+c_2}{u_i+c_1}\right), \quad \text{(A1)}$$

where $\overline{\alpha}_i = (\partial n\alpha/\partial n_i)_{T,P,n_{j\neq i}}$. All quantities appearing in Eq. A1 have been defined in the Introduction. A point of importance is that u_i corresponds to the liquidlike root, obtained by solving the EoS for pure component i, so that φ_i corresponds to the pure component in the liquid state at the mixture T and P. In order to obtain liquidlike values for u_i even at zero pressure, we limit our analysis to systems with components characterized by α_i's that are larger than the limiting value α_{lim} (see Introduction).

On the other hand, the solution of Eq. 1 for $(G^E/RT)^*$, the excess Gibbs free energy obtained from the G^E model, yields

$$\left(\frac{G^E}{RT}\right)^* = -\Sigma x_i \ln\left(\frac{b}{b_i}\right) + q(\alpha) - \Sigma x_i q(\alpha_i), \quad \text{(A2)}$$

where x_i denotes composition in the liquid phase, and q is the approximate form of the $q^e(\alpha)$ used in the development of each one of the MHV2, PSRK, and Soave models. Since

$$\ln \gamma_i = \left[\partial\left(\frac{nG^E}{RT}\right)\Big/\partial n_i\right]_{T,P,n_{j\neq i}},$$

differentiation of Eq. A2 and rearrangement of the resulting terms, leads to

$$\ln \gamma_i^* = -\left[\frac{b_i}{b} - 1 + \ln\left(\frac{b}{b_i}\right)\right] + \left(\frac{dq}{d\alpha}\right)[\overline{\alpha}_i - \alpha] + q(\alpha) - q(\alpha_i). \quad \text{(A3)}$$

Obviously, $\ln \gamma_i^*$ is the activity coefficient obtained from the G^E model used, and corresponds to zero pressure, since the mixing rule Eq. 1 is obtained at the same pressure. Further, $(dq/d\alpha)$ is the derivative with respect to α of the approximate form $q(\alpha)$.

Taking the difference between $\ln \gamma_i$ from Eq. A1 and $\ln \gamma_i^*$ at zero pressure, we obtain

$$\Delta \ln \gamma_i = -(\alpha - \overline{\alpha}_i)\left[\frac{dq^e(\alpha)}{d\alpha} - \frac{dq(\alpha)}{d\alpha}\right] + [q^e(\alpha) - q(\alpha)] - [q^e(\alpha_i) - q(\alpha_i)], \quad \text{(A4)}$$

where $dq^e(\alpha)/d\alpha$ is the derivative of the exact $q^e(\alpha)$. A more complicated equation describes the difference between $\ln \gamma_i$ from Eq. A1 at nonzero pressure and $\ln \gamma_i^*$. However, at low

pressures (say 0.1 or 1 bar, at which the results of Figures 3–6 have been generated), the pressure effect yields a correction factor that, as expected, is negligible compared to the values of $\Delta \ln \gamma_i$ and $\Delta(G^E/RT)$ (as the ones shown in Figures 3–6).

Since $(G^E/RT) = \Sigma x_i \ln \gamma_i$, Eq. A4 easily yields the difference $\Delta(G^E/RT)$ between the excess Gibbs free energy calculated from the EoS and $(G^E/RT)^*$ obtained from the G^E model used:

$$\Delta\left(\frac{G^E}{RT}\right) = \left(\frac{G^E}{RT}\right) - \left(\frac{G^E}{RT}\right)^* = [q^e(\alpha) - q(\alpha)] - \Sigma x_i[q^e(\alpha_i) - q(\alpha_i)]. \quad \text{(A5)}$$

In deriving Eq. A5, the terms containing the derivatives $dq^e(\alpha)/d\alpha$ and $dq(\alpha)/d\alpha$ are eliminated by taking into account the relationship $\alpha = \Sigma x_i \bar{\alpha}_i$.

Manuscript received Sept. 7, 1993, and revision received Apr. 18, 1994.